

Quasiparticle properties of doped quantum-well systems

J. A. White* and J. C. Inkson

University of Exeter, Department of Physics, Stocker Road, Exeter EX4 4QL, United Kingdom

(Received 4 April 1990)

A two-pole model for the inverse dielectric matrix for a doped quantum-well system is developed, including both intraband and interband excitations. Using this model response function, the quasiparticle properties in GaAs quantum wells are investigated within the GW approximation for the electron self-energy. It is found that, for wide wells, intersubband scattering terms contribute significantly to the subband-gap renormalization, effective-mass changes, and quasiparticle lifetimes. It is found that intersubband electron-electron scattering rates may be similar to those for LO-phonon emission, while intrasubband rates can be an order of magnitude higher.

I. INTRODUCTION

The electronic properties of quasi-two-dimensional (2D) systems have been studied extensively both experimentally and theoretically in recent years.¹ In addition to one-electron properties, many-body effects (quasiparticle effective mass and correlation energy) have been studied. In this respect, changes in effective masses and subband renormalization in silicon inversion layers^{1,2} have been of interest, since in this case the 2D electron density can be varied continuously over a wide range and therefore provide the opportunity to test, in some detail, the theory. More recently GaAs/AlAs systems have become the center of attention where, for instance, a single layer of GaAs between two semi-infinite Ga-Al-As slabs produces a 2D quantum well for electrons in the conduction band of the GaAs. In such systems, because of the low GaAs band mass, many-body effects are not expected to be as important as in silicon. However, there are still significant exchange-correlation contributions to the quasiparticle properties.³

The central quantity in any calculation of quasiparticle properties is the electron self-energy. This requires the calculation of the screened electron-electron interaction, which in turn involves the calculation and inversion of the dielectric response function. For homogeneous systems this can be greatly simplified by making use of the well-known plasmon-pole approximation for the inverse dielectric function.⁴ In this approximation, the full spectrum of excitations (plasmons and electron-hole pairs) to which the electrons may couple is replaced by a single branch of effective bosons. The energy and oscillator strength of the effective modes are then determined by fitting to the static response function and to the longitudinal f -sum rule. In the past, plasmon-pole approximations have been employed successfully in the calculation of quasiparticle properties for the three-dimensional electron gas⁴ and, neglecting intersubband excitations, for the quasi-2D electron gas.⁵ Generalized forms of the plasmon-pole approximation have also been applied to the calculation of band-structure properties of semiconductors and simple metals⁶ and to the calculation of

quasiparticle properties in layered 2D electron-gas systems.⁷

The use of the plasmon pole concentrates attention on the plasmons themselves and gives a clear physical picture of the self-energy as due to the virtual exchange of plasmons and the lifetime of the state (given by the imaginary part of the self-energy) as due to plasmon emission. There have been a number of calculations of the plasmon spectrum in quasi-two-dimensional systems using a variety of formalism.^{8,9} The conclusion for the common quantum-well system with one occupied band is that there are as many plasmon bands as there are electronic subbands. The lowest plasmon band is due to intraband and the higher bands are due to interband polarization. The energies of the plasmons are typically of the order of both the intersubband energies and, for typical experimental parameters, optical phonon energies. This, together with the reduced dimensionality, suggests that the self-energy and hence the quasiparticle parameters can be expected to show much more structure than in the case of bulk semiconductors.

The purpose of this paper is to generalize the plasmon-pole approximation to the multiband case in quantum wells in order to both simplify the calculation of the self-energy when intersubband excitations are of importance, and hopefully clarify the physics. In Sec. II the longitudinal f -sum rules for the elements of the inverse dielectric matrix are described for a quantum well with two subbands of importance, and in Sec. III the plasmon-pole approximation is defined. In Sec. IV the model response function is applied to the calculation of quasiparticle properties in GaAs quantum wells. We emphasize the importance of intersubband scattering contributions to the subband-gap renormalization and to quasiparticle lifetimes. Conclusions are presented in Sec. V.

II. MODEL AND SUM RULES

We consider the lowest two subbands, $n=0,1$, of a single modulation-doped semiconductor quantum well of width a within the effective-mass approximation. For simplicity we assume that only the lowest subband is oc-

cupied with an areal electron density N . We also assume that the subband wave functions are those of an infinite square well. This is expected to be a good enough approximation for symmetric quantum wells in the GaAs/Ga_{1-x}Al_xAs system when the barrier height is high compared to the energy gap between the subbands. Electrons exhibit free-particle-like behavior in the plane of the well, with “bare” mass m for each subband. The screening of the Coulomb interaction by the intrinsic semiconductor is described by a dielectric constant κ .

The Hamiltonian for the system then is that of particles in a simple 2D square-well potential interacting via a Coulomb interaction $e^2/\kappa r$. The spatial part of the wave function for the single-particle state with parallel momentum \mathbf{k} , in subband n , is thus

$$\psi_{\mathbf{k}}^n(\mathbf{r}) = \phi_n(z) e^{i\mathbf{k}\cdot\rho}, \quad (1)$$

where $\mathbf{r} = (\rho, z)$ and any \mathbf{k} dependence of the $\phi_n(z)$ is neglected. Denoting the corresponding annihilation operator for spin σ as $c_{\mathbf{k}n\sigma}$, the Hamiltonian may be written

$$H = \sum_{\mathbf{q}, n, \sigma} t_{qn} c_{\mathbf{q}n\sigma}^\dagger c_{\mathbf{q}n\sigma} + \frac{1}{2} \sum_{\substack{\mathbf{q} \neq 0 \\ \mathbf{k}, \mathbf{k}', \sigma, \sigma' \\ l, l', n, n'}} V_q^{ll'nn'} c_{\mathbf{k}+\mathbf{q}l\sigma}^\dagger c_{\mathbf{k}'-\mathbf{q}l'\sigma'}^\dagger c_{\mathbf{k}'n'\sigma'} c_{\mathbf{k}l\sigma}, \quad (2)$$

where $t_{qn} = E_n + q^2/2m$ are the “single-particle” n th subband energies, with minima at $E_0 = 0$ and $E_1 = E_g$,

$$V_q^{ll'nn'} = \frac{2\pi}{\kappa q} \int \int dx dx' \phi_l(x) \phi_l(x') \times e^{-q|x-x'|} \phi_n(x') \phi_n(x') \equiv v_q D_q^{ll'nn'} \quad (3)$$

are the Coulomb matrix elements between subband wave functions $ll'nn'$ for a momentum exchange of $\hbar\mathbf{q}$, $v_q = 2\pi/\kappa q$ is the 2D Fourier transform of the Coulomb interaction, and D is the weighting factor. All other symbols have their usual meaning. In the Hamiltonian (2) we have included all electron-electron interactions beyond the Hartree approximation in the second term.

From the orthonormality of the subband wave functions, it is easy to show that D^{0000} , D^{1111} , $D^{0011} \rightarrow 1$ and $D^{0101} \propto qa$ as $qa \rightarrow 0$, while all of these four terms are proportional to $1/qa$ for $qa \rightarrow \infty$. By symmetry we also have $D^{0001} \equiv D^{1110} \equiv 0$.

The random-phase approximation (RPA) dielectric function for the system is most easily dealt with by considering the Fourier transform in the plane and then expressing it as a matrix in the subband pairs appropriate to the Coulomb matrix elements in Eq. (3), thus

$$\epsilon_{\alpha\beta}(q, \omega) = \delta_{\alpha\beta} - V_q^{\alpha\beta} P_\beta(q, \omega), \quad (4)$$

where the indices α and β are the subband pairs (00),(01),(11). We shall denote such subband pairs with greek letters throughout this paper.

The calculation for the intrasubband polarization P_{00} has been performed by Stern⁸ and for the intersubband term P_{01} we use the formulation of King-Smith and Inkson.⁹ Since only the lowest subband is occupied, $P_{11} \equiv 0$.

The spectrum of excitations is given by the inverse dielectric matrix

$$\text{Im}\epsilon_{\alpha\beta}^{-1}(q, \omega) \neq 0, \quad (5)$$

i.e., intraband electron-hole pairs when $\text{Im}[P_{00}(q, \omega)] \neq 0$, interband electron-hole pairs when $\text{Im}[P_{01}(q, \omega)] \neq 0$, and plasmons when $\det\epsilon_{\alpha\beta}(q, \omega) = 0$.

In this case the plasmon modes are unmixed because of the symmetry, i.e., they are pure intraband and pure interband excitations given by $\epsilon_{0000}(q, \omega) = 0$ and $\epsilon_{0101}(q, \omega) = 0$, respectively. In other words, there are no off-diagonal terms in $\epsilon_{\alpha\beta}(q, \omega)$ so that the inversion is trivial and $\det\epsilon_{\alpha\beta}(q, \omega)$ reduces to $\epsilon_{0000}(q, \omega)\epsilon_{0101}(q, \omega)$.

The intraband plasmon corresponds to charge-density oscillations in the plane of the quantum well and has the well-known $\omega \propto q^{1/2}$ behavior at long wavelengths. The interband plasmon corresponds to charge-density oscillations across the well and its energy tends to a constant value in the $q \rightarrow 0$ limit. The excitation spectrum is shown in Fig. 1 for GaAs parameters ($m = 0.07$, $\kappa = 13$) when the well width $a = 100 \text{ \AA}$, $N = 3.3 \times 10^{11} \text{ cm}^{-2}$, and the subband gap has been chosen as 30 meV. Also note that there is no Landau damping of the intraband plasmons lying within the interband electron-hole continuum due to the symmetry, which ensures that $D^{0001} \equiv D^{1110} \equiv 0$.

Now, in order to make a plasmon-pole-type approximation for the inverse dielectric matrix we require the longitudinal f -sum rules for the individual elements of the inverse dielectric matrix. As we wish to take each subband into account separately, we must consider the operators

$$\rho_{\mathbf{q}}^{nn'} = \sum_{\mathbf{k}, \sigma} c_{\mathbf{k}+\mathbf{q}n\sigma}^\dagger c_{\mathbf{k}n'\sigma} \quad (6)$$

such that the operator denoting the parallel density fluctuations at point z with parallel wave vector \mathbf{q} is

$$\rho_{\mathbf{q}}(z) = \sum_{n, n'} \phi_n^*(z) \phi_n(z) \rho_{\mathbf{q}}^{nn'}, \quad (7)$$

and the real-space density operator is the two-dimensional Fourier transform of this. The double commutators

$$F_q^{ll'nn'} = \langle 0 | [[H, \rho_{\mathbf{q}}^{ll'}], \rho_{-\mathbf{q}}^{nn'}] | 0 \rangle \quad (8)$$

contribute to the oscillator strength sum for the inverse dielectric matrix, where the expectation value is taken over the interacting ground state. This may be seen more clearly by writing

$$F_q^{ll'nn'} = - \sum_s (E_s - E_0) [\langle 0 | \rho_{\mathbf{q}}^{ll'} | s \rangle \langle s | \rho_{-\mathbf{q}}^{nn'} | 0 \rangle + \langle 0 | \rho_{-\mathbf{q}}^{nn'} | s \rangle \langle s | \rho_{\mathbf{q}}^{ll'} | 0 \rangle] \quad (9)$$

(where s are the eigenstates of the Hamiltonian) and comparing with the definition of the density-density correlation function.¹⁰ This allows the sum rules for the inverse dielectric function to be written down as

$$\int_0^\infty \omega \text{Im}\epsilon_{0000}^{-1}(q, \omega) d\omega = - \frac{\pi}{2} V_q^{0000} F_q^{0000}, \quad (10)$$

$$\int_0^\infty \omega \text{Im} \epsilon_{010}^{-1}(q, \omega) d\omega = -\frac{\pi}{2} V_q^{0101} (F_q^{0110} + F_q^{1001}). \quad (11)$$

Unfortunately, expression (8) cannot be evaluated in the general case without, in effect, solving the many-body problem. Instead we restrict ourselves to the calculation of the f -sum rule for the RPA inverse dielectric matrix. This is obtained by replacing the full Hamiltonian in Eq. (8) by the kinetic-energy term only. Then the density-density correlation function becomes just the lowest-order approximation to the polarization and the only nonzero terms of $F_q^{ll'nn'}$ are those with $l=n'$, $l'=n$. In fact, this is just the Hartree-Fock approximation to the inverse dielectric response function. This does not restrict the applicability of the resulting sum rules, however, since it can easily be shown that the Hartree-Fock, RPA, and Hubbard-type dielectric functions¹⁰ satisfy the same longitudinal f -sum rule. Evaluating the commutators we find

$$F_q^{0000} = -\frac{q^2 N}{m}, \quad (12)$$

$$F_q^{0110} = F_q^{1001} = -E_g N - \frac{q^2 N}{2m}, \quad (13)$$

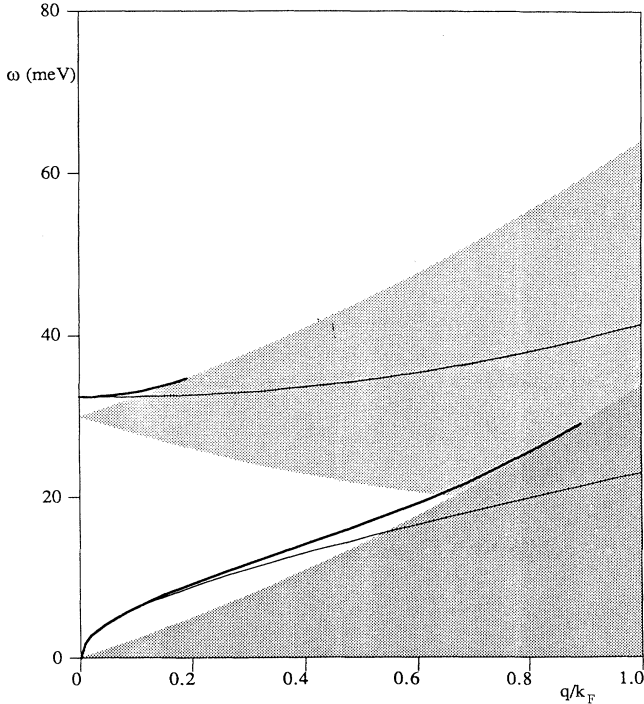


FIG. 1. Plasmon modes (thick lines) of a doped quantum well with $n = 3.3 \times 10^{11} \text{ cm}^{-2}$, well width $a = 100 \text{ \AA}$, $E_g = 30 \text{ meV}$, $\kappa = 13$, and $m = 0.07$. The shaded areas show the intraband and interband electron-hole continua. Also shown (thin lines) are the effective intraband and interband plasmon poles of Eq. (19), which approximate the plasmons for small q and lie inside the electron-hole pair bands for large q .

with all other terms zero. Finally, it also follows that

$$\int_0^\infty \omega \text{Im} \epsilon_{1100}^{-1}(q, \omega) d\omega = -\frac{\pi}{2} V_q^{1100} F_q^{0000}. \quad (14)$$

In the limit $q \rightarrow 0$ these sum rules are exhausted by the plasmon modes. Equations (10) and (14) are the same as those used by Vinter^{2,5} to treat intrasubband excitations, while Eq. (11) describes the total coupling strength to intersubband excitations.

Now we ask how these results are affected if we go beyond the RPA. Suppose only Coulomb terms that do not scatter particles between subbands (i.e., terms of the form V^{llnn}) are included in the Hamiltonian (2) when the double commutator of Eq. (8) is evaluated. This means that all renormalizations of the Green functions due to coupling to intraband excitations are included in Eq. (9). These are expected to be the most important corrections. In this case one finds that the density operators ρ_q^{00} and ρ_q^{11} each commute with the Coulomb potential-energy operator so that the RPA result [Eq. (12)] remains valid. ρ_q^{01} does not commute with the Coulomb potential, however, so that Eq. (13) is not valid at this level of approximation. The correction to F_q^{0110} and F_q^{1001} arising from these terms is independent of q and so appears as a correction to E_g when added to the RPA result [Eq. (13)]. We find

$$\begin{aligned} \delta F_q^{0110} &= \delta F_q^{1001} \\ &= \left\langle 0 \left| \sum_{\substack{\mathbf{k}, \mathbf{k}' \\ \mathbf{q}' \neq 0 \\ \sigma, \sigma'}} (V_{\mathbf{q}'}^{0000} - V_{\mathbf{q}'}^{0011}) \right. \right. \\ &\quad \left. \left. \times c_{\mathbf{k}+\mathbf{q}'0\sigma}^\dagger c_{\mathbf{k}'-\mathbf{q}'0\sigma'}^\dagger c_{\mathbf{k}'0\sigma'} c_{\mathbf{k}0\sigma} \right| 0 \right\rangle. \end{aligned} \quad (15)$$

Here $|0\rangle$ is the ground state for the Hamiltonian containing only Coulomb terms of the form V^{llnn} . Using the Hartree-Fock approximation for $|0\rangle$, only the "exchange term" ($\mathbf{q}' = \mathbf{k}' - \mathbf{k}$) contributes to the sum over \mathbf{q}' . That term proportional to V^{0000} appears as just an average (over the occupied levels) of the exchange energy in the lower subband, while that proportional to V^{0011} must be interpreted as an excitonic correction.

In practice a more exact calculation would start with a self-consistent solution to the electronic states in the quantum well so that most of these corrections are already taken account of in the definition of the energy levels t_{kn} . We shall therefore use Eq. (13) and assume from now on that this renormalization of the energy levels is included in the input value of E_g .

III. PLASMON-POLE APPROXIMATION

For the symmetric quantum well it is sufficient to consider the diagonal elements of the dielectric matrix. Following Ref. 4 we approximate the elements of the inverse dielectric matrix by

$$\epsilon_{\alpha\alpha}^{-1}(q, \omega) = 1 + \frac{\omega_{p\alpha}^2}{\omega^2 - \omega_{q\alpha}^2 + i\delta}. \quad (16)$$

Ensuring that the f -sum rules of Eqs. (10)–(13) are satisfied gives

$$\omega_{p00}^2 = V_4^{0000} F_q^{0000} = \frac{2\pi N}{\kappa m} D_q^{0000} q, \quad (17)$$

$$\omega_{p01}^2 = V_q^{0101} (F_q^{0110} + F_q^{1001}) = \frac{4\pi N D_q^{0101}}{\kappa q} \left[E_g + \frac{q^2}{2m} \right], \quad (18)$$

and the condition that each element be correct in the static limit gives the ‘‘plasmon-pole’’ frequencies

$$\omega_{p\alpha}^2 = \omega_{p\alpha}^2 [1 - \epsilon_{\alpha\alpha}^{-1}(q, 0)]^{-1}. \quad (19)$$

The plasmon poles ω_{q00} and ω_{q01} are shown in Fig. 1 in comparison with the actual (RPA) plasmons. For small q , Eq. (19) gives the same dispersion, to lowest order, as that of the actual plasmon modes. This further implies that the residues of the poles in the inverse dielectric matrix, or equivalently the screened interaction, are the same for the approximate plasmon poles and actual plasmon modes in this $q \rightarrow 0$ limit. For large- q values, the poles approximate the two electron-hole pair bands, with one pole lying in the center of each electron-hole continuum.

For an asymmetric well, for which the matrix elements V^{0001} , etc., are nonzero, the situation is more complicated. It is no problem to obtain the RPA f -sum rules for every element of the inverse dielectric matrix in this more general case if we make use of the fact that

$$\int_0^\infty \omega \text{Im}[\epsilon_{\alpha\beta}^{-1}(q, \omega)] d\omega = - \int_0^\infty \omega \text{Im}[\epsilon_{\alpha\beta}(q, \omega)] d\omega, \quad (20)$$

which follows from the asymptotic form ($\omega \rightarrow \infty$) of the dielectric matrix. There is in this case, however, more than one way to construct a plasmon-pole approximation for which each element of the dielectric matrix satisfies the f -sum rule and also has the correct $\omega=0$ behavior. The simplest is to assume a single-pole form for each element

$$\epsilon_{\alpha\beta}^{-1}(q, \omega) = 1 + \frac{\omega_{p\alpha\beta}^2}{\omega^2 - \omega_{q\alpha\beta}^2 + i\delta}, \quad (21)$$

which is the tight-binding equivalent of the reciprocal space generalized plasmon-pole approximation used by Hybertsen and Louie⁶ to calculate semiconductor-band structures. We shall not go into other possible definitions here, which may be defined analogously to the methods of Refs. 6 and 7, but will instead use Eqs. (16)–(19) to investigate the importance of interband scattering terms to the quasiparticle properties in a symmetric quantum well.

IV. QUASIPARTICLE PROPERTIES

The calculation of the quasiparticle properties involves the evaluation of the self-energy. For the symmetric quantum well, this is diagonal in the subband index and each of the diagonal elements has two contributions, which we label by the band index of the internal Green function:

$$\begin{aligned} \Sigma_{nn}(k, E) &= \frac{i}{8\pi^3} \sum_l \int G_{ll}^0(\mathbf{k} + \mathbf{q}, E + \omega) W_{llnn}(q, \omega) \\ &\quad \times e^{i\omega\delta} d\mathbf{q} d\omega \\ &\equiv \sum_l \Sigma_{nn}^l(k, E) \delta_{nn}, \end{aligned} \quad (22)$$

where G_{nn}^0 is the noninteracting Green function for electrons in subband n and the W_{llnn} are matrix elements of the screened interaction

$$W_{\alpha\beta}(q, \omega) = \sum_\gamma \epsilon_{\alpha\gamma}^{-1}(q, \omega) V_q^{\gamma\beta}. \quad (23)$$

$\Sigma_{nn}^l(k, t_{kn})$ describes the perturbation of the quasiparticle state (\mathbf{k}, n) by its coupling, via the Coulomb interaction, to the states consisting of a quasiparticle in state $(\mathbf{k} + \mathbf{q}, l)$ plus a plasmon of momentum \mathbf{q} .¹¹ Thus the quasiparticle energies are given approximately by

$$E_n(k) = t_{kn} + \Sigma_{nn}(k, t_{kn}). \quad (24)$$

Using the plasmon-pole approximation for the screened interaction, the energy and part of the momentum integrations can be performed analytically resulting in a Coulomb hole term, which involves integration over the whole of two-dimensional momentum space, and a screened exchange term for which integration is over only occupied ‘‘internal’’ states (i.e., $|\mathbf{k} + \mathbf{q}| < k_F$ when $l=0$ only).

For the terms with internal Green function $l=n$, the plasmon in the intermediate states are of intraband type only (i.e., $\omega_q = \omega_{q00}$), while for the terms with $l \neq n$ the plasmon in the intermediate states are of interband type (i.e., $\omega_q = \omega_{q01}$). Physically these correspond to the virtual electron state being in the same or alternate subband respectively, i.e., interband plasmons cause transitions between subbands while intraband plasmons leave the electron in the same subband.

A. Quasiparticle subband renormalization and effective masses

Figure 2 shows, for GaAs parameters, the real part of the self-energy at the quasiparticle peak, i.e., the contributions to the effective exchange correlation potentials as a function of parallel momentum.

First consider the two largest terms Σ_{00}^0 and Σ_{11}^1 , which involve intraband (virtual) scattering processes. The self-energy in the lower subband has, generally, the larger magnitude. This is partly because the Coulomb matrix element is larger, but also because of the screened exchange term which acts only on the lower subband. This means that the effect of exchange and correlation is to increase the subband gap. The other significant feature of these two terms is the sharp downward ‘‘spike’’ at around $k = 1.4k_F$, which occurs at the threshold for an electron to emit plasmons. This is seen in 3D systems as well,⁴ but is more pronounced here because of the reduced dimensionality. This spike is largest in the higher subband because the electron-plasmon scattering is restricted in the lower subband by the Pauli principle.

The other main effect of the screened exchange term

may be seen in the different behavior of Σ_{00}^0 and Σ_{11}^1 for $k < k_F$. Screened exchange reduces the energy of states inside the Fermi circle and this effect increases with increasing density. For sufficiently high densities then, Σ_{00}^0 is an increasing function of k for small k , whereas Σ_{11}^1 is always a decreasing function of k for small k .

The terms Σ_{00}^1 and Σ_{11}^0 involve intersubband scattering. These terms are much smaller than the intraband scattering contributions because of the smaller Coulomb matrix elements. Again, each term has a peak corresponding to the threshold for emission of the effective intersubband plasmons. These are just visible at $k \approx 1.1k_F$ for Σ_{11}^0 and $k \approx 2.3k_F$ for Σ_{00}^1 . Note that Σ_{00}^1 is usually negligible because there is no exchange contribution and also because of the large energy separation between the states coupled by the interaction. In Σ_{11}^0 it is bare exchange that is the dominant contribution. This is strongly dependence on the well width through its dependence on the Coulomb matrix element V^{0101} .

Figure 3 shows the exchange-correlation correction to the subband gap as a function of electron density, with and without the effect of intersubband scattering, for two values of the well width. Here the gap has been evaluated at the Fermi wave vector. Note that the interband terms cause a decrease in the subband gap which, in this case, cancels by about 30% the correction from intraband scattering. This reduction is seen to be relatively more important for the larger well width. The largest value of

N plotted here corresponds to $E_F = E_g$, i.e., the higher density for which only the lowest subband is occupied. It should be noted that the results for the exchange-correlation correction to the subband energies cannot be compared directly with experiment since we do not have the Hartree potential. However, it can be seen that if a comparison of theory and experiment is to be made, then this will require the inclusion of intersubband scattering effects in the exchange-correlation potential. Another interesting point would be to compare the results of many-body perturbation theory with those of density-functional theory, in order to investigate to what extent these intersubband scattering processes are included in a density-functional approach.

The quasiparticle effective mass m^* , which is defined in terms of the quasiparticle group velocity v_g at the Fermi surface, is given by

$$\frac{1}{m^*} = \frac{1}{m} + \frac{1}{k_F} \frac{d}{dk} \text{Re}\Sigma_{00}(k, t_{k0})|_{k=k_F}. \quad (25)$$

This can easily be calculated to the desired accuracy by numerical differentiation of the self-energy. From Fig. 2 we saw that the interband scattering contribution Σ_{00}^1 to the self-energy is very small and is, moreover, a very flat function of k in the region $k \approx k_F$. Its effect on m^* is therefore negligible, as was also shown by Ohkawa² for silicon inversion layers. The behavior of m^* is therefore determined by the intraband term in the self-energy Σ_{00}^0 .

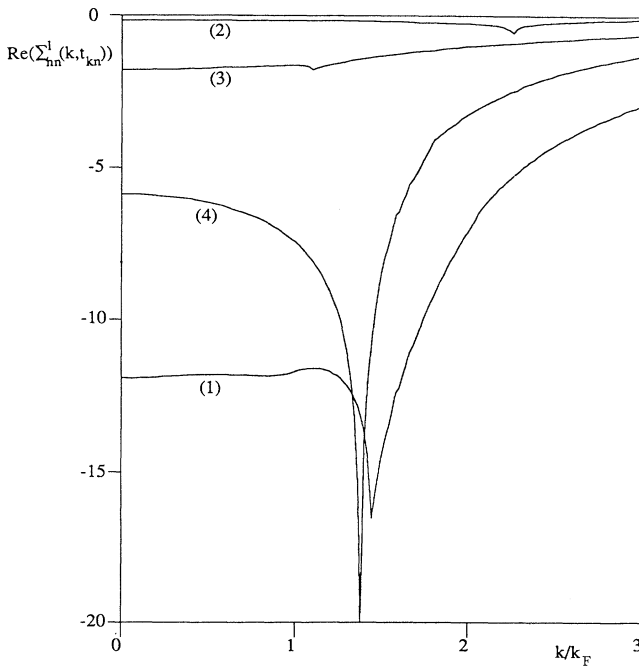


FIG. 2. Real part of the contributions to the self-energy, evaluated at the quasiparticle peak, as a function of k . Σ_{00}^0 [line (1)], Σ_{00}^1 [line (2)], Σ_{11}^0 [line (3)], and Σ_{11}^1 [line (4)], as defined by Eq. (22), are shown. Here $N = 6.4 \times 10^{11} \text{ cm}^{-2}$, $E_g = 30 \text{ meV}$, and $a = 100 \text{ \AA}$.

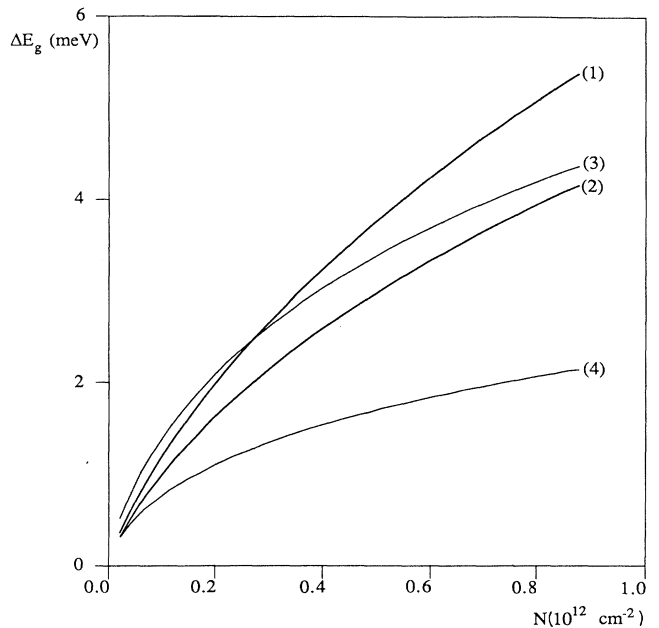


FIG. 3. Self-energy contributions to the subband gap ΔE_g , evaluated at $k = k_F$, as a function of electron density N , shown for $a = 50 \text{ \AA}$, excluding interband scattering [line (1)] and including interband scattering [line (2)]; also for $a = 200 \text{ \AA}$, excluding interband scattering [line (3)] and including interband scattering [line (4)].

Figure 4 shows m^* as a function of electron density N for two values of well width, $a=50$ and 200 Å. The general behavior of m^*vN that we see is in agreement with previous calculations;^{1,2} the effective mass is higher than the bare mass at low electron density and drops rapidly with increasing electron density to a value below the bare value. The variations are in the region of less than or equal to 10% in the density range considered. Notice that m^* is significantly lower for the wider well. This is because the short-range part of the interaction is reduced in wide wells, which increases the importance of exchange effects (which tend to reduce m^*) while reducing the electron-plasmon coupling strength [see Eq. (17)].

It should be noted that for a simple well, like a 3D electron gas, the Fermi level lies away from the region in which the self-energy is varying rapidly. This restricts the possible size of the mass changes [Eq. (25)]. For double wells where coupling between plasmons can be important, this is not necessarily the case and a larger change can result.¹²

B. Quasiparticle lifetime

In a quantum-well system the quasiparticle lifetime is governed by the possibility of the excitation of plasmons, phonons, or electron-hole pairs. In our present model system phonons are neglected and in the plasmon-pole approximation the electron-hole excitations have been subsumed. Calculations using the full RPA response

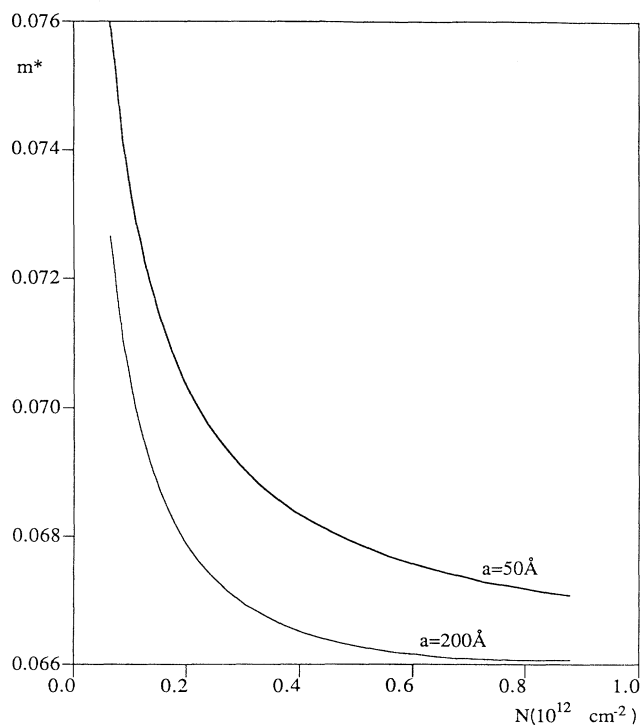


FIG. 4. Quasiparticle effective mass m^* as a function of electron density for well widths $a=50$ and 200 Å.

function show the effect of these to be small anyway, so what we are concerned with here is the magnitude of the lifetime compared to that expected from the low-energy bulk value, which is dominated by phonon emission.

Mathematically, the inverse lifetime for quasiparticles of momentum k in subband n due to scattering into subband n' is given by

$$\tau_{knn'}^{-1} = -2 \text{Im} \Sigma_{nn'}^{n'}(k, t_{kn}) . \quad (26)$$

Like any real scattering process, energy and momentum must be conserved. This gives a well-defined threshold for emission and hence a sharp structure for the lifetime as a function of quasiparticle state. Results for the inverse lifetimes due to intrasubband scattering (the emission of an intraband plasmon) as a function of quasiparticle momentum k , τ_{k00}^{-1} , and τ_{k11}^{-1} , are shown in Fig. 5 for an electron density $N=6.4 \times 10^{11} \text{ cm}^{-2}$ and for well widths $a=50$ and 200 Å. The inverse lifetime has been plotted in units of energy, with 6.5 meV corresponding to 10^{13} s^{-1} .

Since the Coulomb matrix elements for intraband scattering are reduced as well width increases, the larger well width corresponds to a lower emission threshold and

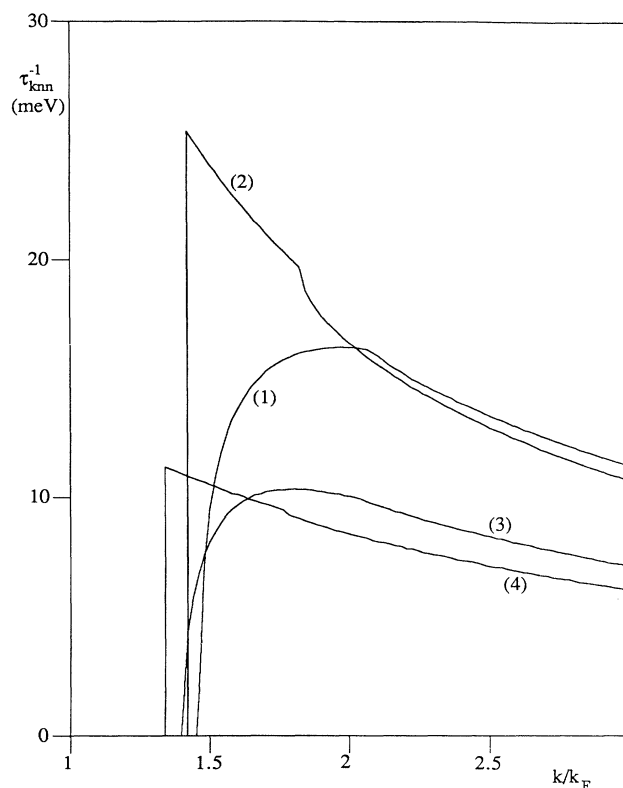


FIG. 5. Inverse lifetime τ_{knn}^{-1} to intrasubband scattering within subband n as a function of quasiparticle parallel momentum k . Plotted for both subbands and for two well widths: $n=0$, $a=50$ Å [line (1)]; $n=1$, $a=50$ Å [line (2)]; $n=0$, $a=200$ Å [line (3)]; $n=1$, $a=200$ Å [line (4)]. Here $N=6.4 \times 10^{11} \text{ cm}^{-2}$ and $E_g=30 \text{ meV}$.

also to a reduced scattering rate. The discontinuous change in the intraband scattering rate in the higher subband is typical of scattering from plasmons in a two-dimensional electron gas.¹³ This discontinuity is not seen for intraband scattering within the lowest subband, however, because of the restrictions of the exclusion principle on scattering.

Figure 6 shows the intersubband scattering rates, again for $N = 6.4 \times 10^{11} \text{ cm}^{-2}$ and for two values of well width, $a = 50$ and 200 \AA . The subband gap has been taken as $E_g = 30 \text{ meV}$. Of course, the threshold for the process $0 \rightarrow 1$ (emission of an n interband plasmon together with excitation to the higher band) is much higher than that for the process $1 \rightarrow 0$ in which the electron falls to the lower subband. The largest effect, however, is that the intersubband scattering rate is much larger for the wider well. At $a = 50 \text{ \AA}$ the interband scattering rate is only about 1% of the intraband rate whereas at $a = 200 \text{ \AA}$ this has increased to about 10%. This ratio increases still further for larger well widths, although for $a > 500 \text{ \AA}$ both intraband and interband scattering rates are decreasing functions of well widths as all Coulomb matrix elements fall off as $1/a$ for $qa \gg 1$.

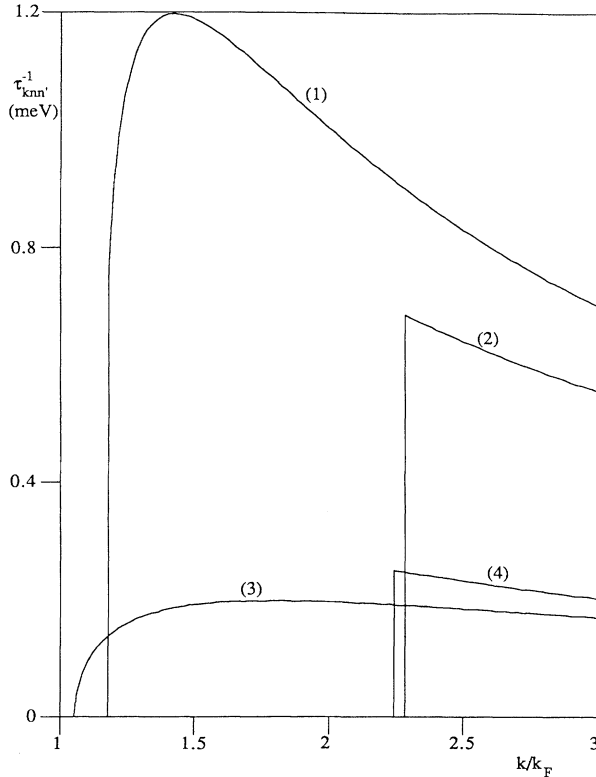


FIG. 6. Inverse lifetime $\tau_{knn'}^{-1}$ to intersubband scattering from subband n to subband $n' \neq n$, as a function of quasiparticle parallel momentum k . Plotted for both subbands n and for two well widths: $n = 1, n' = 0, a = 200 \text{ \AA}$ [line (1)]; $n = 0, n' = 1, a = 200 \text{ \AA}$ [line (2)]; $n = 1, n' = 0, a = 50 \text{ \AA}$ [line (3)]; $n = 0, n' = 1, a = 50 \text{ \AA}$ [line (4)]. Again $N = 6.4 \times 10^{11} \text{ cm}^{-2}$ and $E_g = 30 \text{ meV}$.

As for the real part of the self-energy, we find that the τ_{k10}^{-1} is almost independent of the input value of E_g . This is because the effect of the energy shift appearing in the screened interaction and in the Green functions (i.e., the changes in the interband plasmon energy and the band gap) largely cancel. As expected, τ_{k01}^{-1} is strongly dependent on E_g , with the threshold wave vector increasing and the scattering rate decreasing as E_g increases. Here the same subband gap $E_g = 30 \text{ meV}$ has been used for both $a = 50$ and 200 \AA , thereby isolating the effect of the Coulomb matrix element. In reality, as d decreases, E_g increases, so that the importance of τ_{k01}^{-1} is reduced still further for narrow wells.

For the electron density considered here, the rate for intrasubband scattering via the Coulomb interaction is large compared with other scattering processes, such as scattering from LO phonons.¹⁴ It is also found that intraband Coulomb scattering corresponds to large momentum transfers (approximately k_F) so that it is an effective channel for momentum relaxation. It is therefore expected to be the dominant scattering process in hot-electron transport. The intersubband scattering rate ($1 \rightarrow 0$), although much lower than the intrasubband rate, is still significant. From Fig. 1 it is apparent that, because interband plasmons exist only for small wave vectors, interband scattering is predominantly due to emission of electron-hole pairs. For $a = 200 \text{ \AA}$, however, the intersubband lifetime of about 10^{-12} s is still similar to that for interband relaxation by LO-phonon emission.¹⁵ It might therefore be expected that electron-electron interactions will also become the dominant intersubband relaxation process inside wells for which the subband gap is small enough to restrict LO-phonon emission.

These Coulomb scattering rates, both intraband and interband, increase as electron density increases. From the fact that residue of the screened interaction at the plasmon pole (i.e., the square of the electron-plasmon coupling matrix element) scales as ω_p^2/ω_q , the dependence of scattering rate on electron density may be estimated. Using Eqs. (17)–(19), we find that the intraband scattering rate scales approximately as between $N^{1/2}$ and N , while the interband scattering rate scales approximately as N .

V. CONCLUSIONS

The screened interaction quasiparticle properties of a symmetric doped quantum well, including two subbands with only the lowest occupied, have been considered. A longitudinal f -sum rule has been derived for the elements of the inverse dielectric matrix. This derivation is restricted to the RPA, although the result is also valid for Hubbard-type dielectric functions and is expected to be a good approximation for the exact sum rule. A plasmon-pole approximation to the screened interaction is then defined which satisfies this f -sum rule and which treats intraband and interband excitations separately. For the symmetric well these modes are unmixed by symmetry. For an asymmetric well the f -sum rule for the RPA inverse dielectric matrix follows from Eqs. (4) and (20) so that a generalized plasmon-pole approximation could

also be constructed in this case. This approximation to the screened interaction was then applied to the calculation of quasiparticle properties in GaAs quantum wells.

We have seen that the positive exchange-correlation contribution to the subband gap due to intraband scattering is partially canceled by the negative contribution from intersubband scattering, which is predominantly due to the bare exchange energy in the higher subband. This cancellation is largest for wide wells for which the intersubband Coulomb matrix element is relatively larger. Further, the subband-gap correction was found to be only weakly dependent on the first approximation for the gap.

Intersubband effects were found to be negligible for the quasiparticle effective mass m^* , although m^* is strongly dependent on well width through its effect on the Coulomb matrix elements. Electron-electron interactions cause m^* to increase as well width decreases, which, in

GaAs/AlAs systems, adds to the one-electron effects of confinement and nonparabolicity which also tend to increase m^* as well width decreases.

The quasiparticle lifetime to intrasubband and intersubband scattering has also been calculated. While the exact form of scattering rate as a function of quasiparticle momentum is not expected to be given accurately (in particular losses to electron-hole pair excitations are not treated correctly), the magnitude of the scattering rates should give a good account of the importance of the various scattering processes. For typical 2D electron densities, intrasubband scattering rates are large and are expected to be the dominant relaxation process for hot electrons: Relative to intrasubband scattering rates, intersubband scattering was found to be small, especially in narrow wells. The intersubband scattering rates are, however, significant and may be comparable to the intersubband transition rate via LO-phonon emission.

*Present address: Department of Theoretical Physics, University of Lund, Sölvegatan 14A, S-22362 Lund, Sweden.

¹T. Ando, A. B. Fowler, and F. Stern, *Rev. Mod. Phys.* **54**, 437 (1982).

²J. L. Smith and P. J. Stiles, *Phys. Rev. Lett.* **29**, 102 (1972); C. S. Ting, T. K. Lee, and J. J. Quinn, *ibid.* **34**, 870 (1975); F. J. Ohkawa, *Surf. Sci.* **58**, 326 (1976); B. Vinter, *Phys. Rev. B* **13**, 4447 (1976).

³G. Kawamoto, R. Kalia, and J. J. Quinn, *J. Surf. Sci.* **98**, 589 (1980); T. Ando, in *Third Brazilian School of Semiconductor Physics*, edited by C. E. T. Gonçalves da Silva, L. E. Oliveira, and J. R. Leite (World Scientific, Singapore, 1987).

⁴B. I. Lundqvist, *Phys. Kondens. Mater.* **6**, 193 (1967); **6**, 206 (1967); A. W. Overhauser, *Phys. Rev. B* **3**, 1888 (1971).

⁵B. Vinger, *Phys. Rev. B* **15**, 3947 (1977).

⁶M. S. Hybertsen and S. G. Louie, *Phys. Rev. Lett.* **55**, 1418 (1985); J. E. Northrup, M. S. Hybertsen, and S. G. Louie, *Phys. Rev. Lett.* **59**, 819 (1987); W. von der Linden and P.

Horsch, *Phys. Rev. B* **37**, 8351 (1988); J. A. White and J. C. Inkson, *Solid State Commun.* **66**, 371 (1988).

⁷J. A. White and J. C. Inkson, *Semicond. Sci. Technol.* **4**, 724 (1989).

⁸F. Stern, *Phys. Rev. Lett.* **18**, 546 (1967).

⁹D. Dahl and L. J. Sham, *Phys. Rev. B* **16**, 651 (1977); A. Eguluz and A. Maradudin, *Ann. Phys. (N.Y.)* **113**, 29 (1978); A. Tselis and J. J. Quinn, *Surf. Sci.* **113**, 362 (1982); R. D. King-Smith and J. C. Inkson, *Phys. Rev. B* **33**, 5489 (1986).

¹⁰G. D. Mahan, *Many-Particle Physics* (Plenum, New York, 1981), Chap. 5.

¹¹T. M. Rice, *Ann. Phys. (N.Y.)* **31**, 100 (1965).

¹²J. A. White and J. C. Inkson (unpublished).

¹³P. Hawrylak, G. Eliasson, and J. J. Quinn, *Phys. Rev. B* **37**, 10 187 (1988).

¹⁴B. A. Mason and S. Das Sarma, *Phys. Rev. B* **35**, 3890 (1987).

¹⁵B. K. Ridley, *Phys. Rev. B* **39**, 5282 (1989); M. C. Tatham, J. F. Ryan, and C. T. Foxon, *Phys. Rev. Lett.* **63**, 1637 (1989).